Hindawi
International Journal of Aerospace Engineering
Volume 2019, Article ID 2592189, 16 pages
https://doi.org/10.1155/2019/2592189

Research Article

PB: A Message Transmission Method Based on Area Layer Division in UAV Networks

Lisong Wang[1], **Feifei Zhu**[1], **Qing Zhou**[2], **Kui Li**[2] **and Liang Liu**[1]

[1]*College of Computer Science and Technology, Nanjing University of Aeronautics and Astronautics, 29 Jiangjun Avenue, Nanjing 210016, China*
[2]*National Key Laboratory of Science and Technology on Avionics Integration, China Aeronautical Radio Electronics Research Institute, Shanghai 200233, China*

Correspondence should be addressed to Lisong Wang; wangls@nuaa.edu.cn

Received 27 June 2019; Revised 22 September 2019; Accepted 5 October 2019; Published 11 November 2019

Academic Editor: Antonio Concilio

A search and rescue mission is a typical UAV network application scenario. In this case, it is necessary to deliver messages quickly and efficiently to the ground station through mutual cooperation between UAVs. Many methods used in this case have problems such as unbalanced *popularity* (the ratio of the relayed message number to the total message number) of nodes, large proportion of ping-pong effect, and long delay. In view of the above problems, this paper proposes a method named PB (*Popularity* Balance Method for UAVs in the same area layer) based on division of the whole search area. The method divides the search area into multiple area layers. Message transmission between area layers adopts a geographical routing manner, that is, messages are transmitted to the area layer closer to the ground station. The division of the search area changes the pattern of message transmission. Messages are delivered to the area layer closer to the destination node rather than the node closer to the destination. The pattern causes messages' passing direction to be replaced by "point-to-point closer" to "point-to-face closer." On the basis of message transmission at area layers, reasonable planning of UAVs' distribution can effectively improve the network performance deterioration caused by a "hot spot." Both analysis and experiments show that PB is superior to some existing methods in *popularity* balance of nodes and ping-pong effect. In addition, experiments also show that it gets better results in targets of delay, delivery rate, and hop count.

1. Introduction

The UAV is a hotspot in the new round of scientific and technological revolution and industrial revolution in the world, and its industrial development is related to national interests [1]. For many tasks, unmanned units are often required to work together to complete a task [2]. At this point, according to the characteristics of the task scene and the characteristics of the unmanned unit network, how to use the appropriate routing method to transfer messages to the destination node becomes an important technical problem [3].

UAVs establish high-throughput links through wireless transmission to form a temporary, multihop regional connection, which is a mobile ad hoc network [4]. However, due to the high-speed continuous movement of drones, the network topology of drones changes frequently. When traditional MANET routing methods were used in UAVs, a series of problems occurred, such as low delivery rate and long delay, greatly affecting network performance [5].

Therefore, it is necessary to put forward higher requirements for UAV network routing strategy and conduct relevant researches in a targeted manner. At present, in many situations where UAVs are used, task-driven UAVs are employed [6], and the trajectory of the drone is artificially planned in advance. The drones can only move according to the planned trajectory [7]. For the classic scenario—search and rescue [8]—many existing methods use the idea of geographic routing [9] and delay-tolerant network (DTN) routing algorithms [10]. According to analyzing the characteristics of the scene, messages are transmitted to the

direction closer to the ground station and are allowed to be stored and carried during transmission. These methods are likely to cause some specific drones to consume a lot of energy for transmitting messages, which will constrain them from completing other tasks [11].

In view of the above problems, by analyzing the characteristics of the investigation and rescue mission—the greater regularity of the investigation area—this paper divides the investigation area into multiple regional layers and at the same time uses the idea based on geographic routing to transmit the message to the area near the ground station. The drone node in the middle causes the message to be transmitted closer to the ground station. Due to the uniformity of the distribution of the drones in the scene, the number of messages passing through the drones in each area layer tends to be balanced, which can effectively avoid the appearance of a "hot spot" and improve poor network performance due to the "hot spot." In addition, when the detection area is far away from the ground station, the message at the nearest regional layer of the ground station is transmitted to the ground station by means of the idea of relaying by the drone, which avoids the back-and-forth movement between a UAV and the ground station. The method also effectively avoids the ping-pong effect generated by the back-and-forth transmission of the message, so as to reduce delay.

2. Related Work

In view of the frequent changes of network topology of UAVs, many researchers have studied it. The routing methods mainly include the following:

(1) *Traditional Mobile Ad Hoc Network (MANET) Routing Algorithms.* The traditional routing protocol OLSR is applied in the network of two microaircrafts and ground stations in [12]. The results show that traditional routing protocols cannot cope with rapidly changing topologies [13]. The main reason is that UAVs move extremely fast and the establishment and breakdown of the communication link is extremely frequent, which causes the network topology to change extremely fast [14]. The traditional mobile ad hoc routing protocol does not have a definite time to converge [15], so the transmission efficiency is low

(2) *DTN Routing Algorithms.* Since messages are allowed to be stored and carried, another method is based on a DTN network. DTN routing algorithms are suitable for intermittent connection [10]. Pure DTN routing methods such as epidemic routing [16] often use a multicopy mechanism. One message is copied to the neighbor nodes as often as possible, so that the message can reach the destination node as soon as possible. In [17], R3 is a special case of epidemic routing, which leverages replication to improve delay. In [18], a forwarding mechanism for FANETs is proposed to reduce redundant broadcasts and collisions, thus improving the end-to-end delay and packet delivery ratio. A multicopy mechanism always causes network congestion; thus, excessive messages are congested on the UAV waiting for transmission, which increases delay, so this type of method causes unnecessary copies of messages in the UAV network [19]

(3) *Geographic Routing Algorithms.* Another idea is to transmit messages in a direction closer to the target node based on geographic routing [20]. In [21], GeoDTN+Nav is proposed for ground vehicles; thus, navigation information and the store-carry-forward concept are leveraged. In [14], GPMOR, a geography-based routing protocol, is proposed to address the issue of link interruption due to high mobility by selecting the optimal next hop, but it has a low degree of autonomy. In [22], DTN_{geo} is proposed for UAVs, which is combined with geographic routing and a DTN algorithm. DTN_{geo} uses a single-copy mechanism to ensure that only one copy of any message exists in the network, and forwards the message to a neighbor node that is closer to the destination in space. If there is no neighbor node closer to the ground station, the message will be carried. When the method is used in a search and rescue scene, messages are always transmitted to the specific drone node closest to the ground station, which makes the number of messages passing through this UAV much larger than others, forming the so-called "hot spot." The emergence of a "hot spot" will bring many hazards. Firstly, for the energy-limited UAV, the "hot spot" UAV will consume more energy for message transmission, making the UAV consume too much energy, which will constrain the UAV from completing other tasks. In addition, for the whole UAV network, a large number of messages are congested on the "hot spot" waiting for transmission. The congestion not only easily causes packet loss but also increases the waiting time of message transmission, which can result in the reduction of the delivery rate and the increase of delay. In [22], another two heuristic algorithms, DTN_{close} and DTN_{load} are also proposed to improve network transmission performance. DTN_{close} additionally considers the position information of the drone after a fixed time interval F on DTN_{geo}. The neighbor node closest to the destination node after F time is selected as the next node. DTN_{load} additionally considers the load condition of the node in DTN_{geo}. According to the number of messages to be transmitted by the neighbor node and the message transmission capability in the F time interval, the transmission efficiency of the message to the F time is the highest and the ratio is higher. This is the node whose current node is closer to the destination node. DTN_{close} and DTN_{load} have a certain improvement on the message delivery rate and the ping-pong effect, but experimental results also show that there is still room for optimization in terms of delivery rate, ping-pong effect ratio, and delay

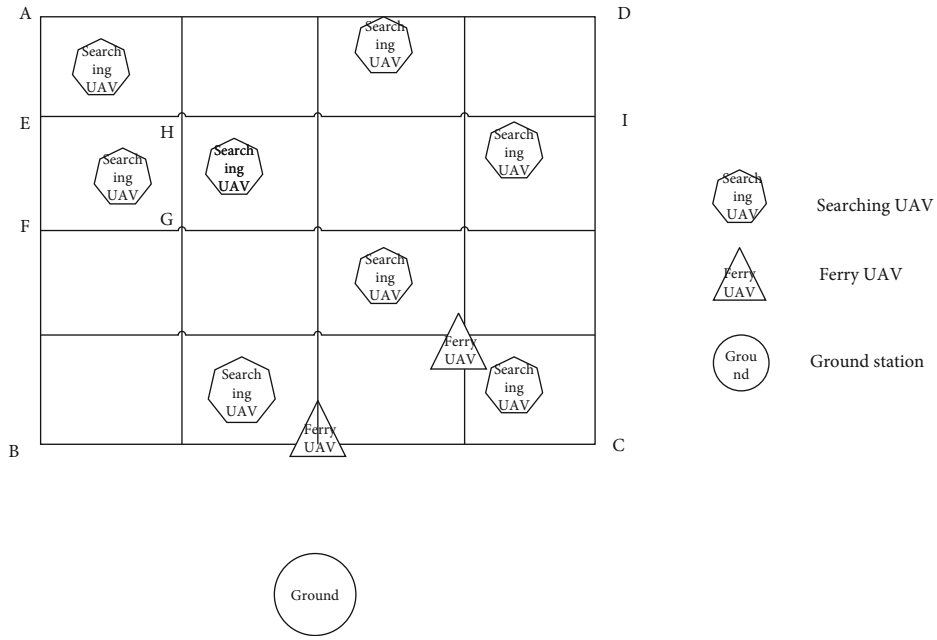

Figure 1: Example of a search and rescue scenario with UAVs.

3. A UAV Message Transmission Method Based on Area Layer Division

In this section, we elaborate on the proposed PB and compare it to other methods of related models. Firstly, we model UAV networks, mainly including the search and rescue scene model, the mobility model, and the rules of area layer division, the message transmission methods between area layers, and the rules of ferry UAVs. Secondly, we describe models of *popularity* balance and ping-pong effect, and we analyze the properties between PB and DTN_{geo}, DTN_{close}, and DTN_{load} on these two models. Finally, we theoretically analyze the advantages of PB compared with DTN_{geo}, DTN_{close}, and DTN_{load}.

3.1. Modeling UAV Networks

3.1.1. Modeling Case Scenario—Search and Recuse. For a typical scene—search and rescue—the target person is waiting to be rescued in the search area. If the search area is large, artificially invested on-site investigation can cause a large amount of human and financial losses because of the unknown geographical situation. Meanwhile, using a unit of UAVs can greatly reduce the loss [23]. UAVs need to collect the picture message in the search area, and transmit collected messages to the ground station as soon as possible. Then, related people in the ground station can piece together the topography in the area to find the location of the target person, and seek the fastest and safest way to save. This task is completely controlled by the ground station, so the trajectory and allocation of drones are all arranged in advance [24].

Since the communication range of UAVs and the ground station are all limited, drones cannot directly establish communication links with the ground station when they are far away from the ground station. Admittedly, flying back to the ground station is a simple, but power-hungry solution that does not scale well. Observing UAVs should use their scarce battery power on mission-driven tasks instead of consuming it by moving closer to the transmission peer (in a testbed of quadcopters, we measured a power consumption of about 200-250 Watts for autonomous flight; the dominating factor is the mechanical part of the copter [25]). Similarly, dense placement of relay UAVs for maintaining connectivity is a possible solution; however, this solution comes at high deployment and operational costs. By introducing ferry nodes to establish connectivity, most of the UAVs may search while the ferries move data physically before transmitting. Note that every UAV in the network may additionally relay messages when possible, including the searching UAVs. It is a plan that takes into account the energy and drone resources.

In a multi-UAV system, the specific functions of searching UAVs and ferry UAVs are as follows:

(1) *Searching UAV*: collecting pictures and also acting as a relay for message transmission

(2) *Ferry UAV:* acting only as a relay, to help searching UAVs quickly transmit messages to the ground

This article uses a rectangular search area as an illustration, as shown in Figure 1.

Here, the Ground is responsible for the planning and analysis of the entire task. Before a task, people in the ground station divide all of the search area into multiple parts and plan the running track of UAVs. During the task, the operation track and running direction of drones are controlled by the control signal. In addition, when messages are returned, the ground station needs to parse them, piece them together to find the location of the target person, and find a suitable search and rescue path.

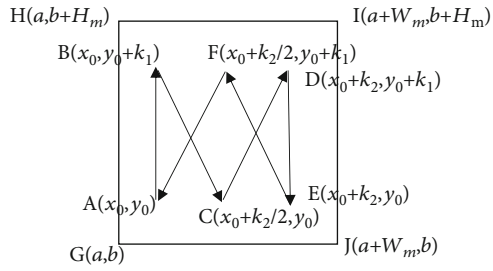

Figure 2: UAV mobility model.

In addition, the relevant areas can be divided into three categories, and the relevant definitions are described as follows:

(1) *Search area (abbreviated as SA)*: the entire area to be investigated, which is shown as ABCD in Figure 1, where height is represented as H_{all} and width is represented as W_{all}

(2) *Area layer (abbreviated as AL)*: multiple subarea layers of the entire search area according to the hierarchy, which is shown as AEID in Figure 1

(3) *Subsearch area* (abbreviated as SSA): the area of each drone's searching part, which is shown as EFGH in Figure 1, where height is expressed as H_m and width is expressed as W_m

These three types of areas are related to each other. If area(SA), area(AL), and area(SSA) are used to represent the area of SA, AL, and SSA, the following relationships are satisfied:

(1) $\sum \text{area(AL)} = \text{area(SA)}$, that is, the sum area of all area layers is the area of the search area

(2) $\sum \text{area(SSA)} = \text{area(SA)}$, that is, the sum area of all subsearch areas is the area of the search area

(3) Let AL_i be the No. i AL, $\text{sum}(i)$ be the number of searching UAVs in the AL_i, SSA_j is the area of No. j UAV in AL_i, and then $\sum_{j=1}^{\text{sum}(i)} \text{area}(\text{SSA}_j) = \text{area}(\text{AL}_i)$, that is, the sum area of all subsearch areas in the same area layer is the area of that area layer

Additionally, in order to perform the mission faster and easier, the following requirements should be met when designing the drones' trajectory [26]:

(1) The number of UAVs in each area layer tends to be the same

(2) The size and shape of each SSA tend to be the same

(3) The trajectory of drones tends to be the same

3.1.2. UAV Mobility Model. The motion of the drone can be described as a linear, directional movement model [13], and the trajectory of the drone is determined by the ground station when performing the investigation-search and rescue mission [27]. For the convenience of description, this paper selects straight flight as the trajectory of each drone in a real scene, as shown in Figure 2.

We describe the subsearch area as a rectangle. The entire area GHIJ is the detection module of each drone. Let H_m be the height of the subsearch area in y-axis, W_m be the width of the subsearch area in the x-axis direction, and R_g be the maximum perception of the sensor on the drone. In order to ensure that all UAVs can complete the investigation of the entire area, it must be ensured that the area of each UAV's investigation is not less than the subsearch area, that is, the detection range covered by the movement track of each UAV is not less than the subsearch area. Therefore, the following constraints must be met between the drone and the reconnaissance module:

$$\begin{cases} \sqrt{(x_0 - a)^2 + (y_0 - b)^2} \le R_g, \\ \sqrt{(x_0 + k_0 - a - W_m)^2 + (y_0 + k_1 - b - H_m)^2} \le R_g. \end{cases} \tag{1}$$

When the above constraint (1) is satisfied, the drone can complete the investigation of the entire module. The drone selects a point as the starting position, and we take the point $\text{A}(x_0, y_0)$ as the starting point as an example for the description. It moves along the AB direction through the k_1 distance to point $\text{B}(x_0, y_0 + k_1)$. The direction of motion begins to move along BC to point $\text{C}(x_0 + k_2/2, y_0)$, reaching point C again to change direction along the CD motion, and to point $\text{D}(x_0 + k_2, y_0 + k_1)$ again to change direction to point $\text{E}(x_0 + k_2, y_0)$. Thus, after changing the direction of motion multiple times, the drone will complete the task of detecting the entire module via $\text{A} \to \text{B} \to \text{C} \to \text{D} \to \text{E} \to \text{F} \to \text{A}$. The position of the drone at each moment is related to its initial position (x_0, y_0) and moving speed v and direction of motion, giving the relationship between the position (x, y) of the drone and time t (where t_0 is just the point when the task is changed in the running direction):

(1) Movement equation along the AB direction: when a drone moves in the AB direction, the task time is represented as $t \in [0, (k_1/v))$; let $t_0 = 0$, and the equation of motion at this period is as follows:

$$\begin{cases} x = x_0, \\ y = y_0 + v \cdot (t - t_0) \end{cases} \tag{2}$$

(2) Movement equation along the BC direction: when a drone moves in the AB direction, the task time is represented as

$$t \in \left[\frac{k_1}{v}, \frac{k_1}{v} + \sqrt{k_1^2 + \left(\frac{k_2}{2}\right)^2} \right) \tag{3}$$

let

$$t_0 = \frac{k_1}{v} \tag{4}$$

the equation of motion at this period is as follows:

$$\begin{cases} x = x_0 + \dfrac{k_2 \cdot v \cdot (t - t_0)}{2\sqrt{k_1^2 + (k_2/2)^2}}, \\ y = y_0 + k_1 - \dfrac{k_1 \cdot v \cdot (t - t_0)}{\sqrt{k_1^2 + (k_2/2)^2}} \end{cases} \tag{5}$$

(3) Movement equation along the CD direction: when a drone moves in the CD direction, the task time is represented as

$$t \in \left[\frac{k_1}{v} + \sqrt{k_1^2 + \left(\frac{k_2}{2}\right)^2}, \frac{k_1}{v} + 2\sqrt{k_1^2 + \left(\frac{k_2}{2}\right)^2} \right) \tag{6}$$

let

$$t_0 = \frac{k_1}{v} + \sqrt{k_1^2 + \left(\frac{k_2}{2}\right)^2} \tag{7}$$

the equation of motion at this period is as follows:

$$\begin{cases} x = x_0 + \dfrac{k_2}{2} + \dfrac{k_2 \cdot v \cdot (t - t_0)}{2\sqrt{k_1^2 + (k_2/2)^2}}, \\ y = y_0 - \dfrac{k_1 \cdot v \cdot (t - t_0)}{\sqrt{k_1^2 + (k_2/2)^2}} \end{cases} \tag{8}$$

(4) Movement equation along the DE direction: when a drone moves in the DE direction, the task time is represented as

$$t \in \left[\frac{k_1}{v} + 2\sqrt{k_1^2 + \left(\frac{k_2}{2}\right)^2}, \frac{2k_1}{v} + 2\sqrt{k_1^2 + \left(\frac{k_2}{2}\right)^2} \right) \tag{9}$$

let

$$t_0 = \frac{k_1}{v} + 2\sqrt{k_1^2 + \left(\frac{k_2}{2}\right)^2} \tag{10}$$

the equation of motion at this period is as follows:

$$\begin{cases} x = x_0 + k_2, \\ y = y_0 + k_1 - v \cdot (t - t_0) \end{cases} \tag{11}$$

(5) Movement equation along the EF direction: when a drone moves in the EF direction, the task time is represented as

$$t \in \left[\frac{2k_1}{v} + 2\sqrt{k_1^2 + \left(\frac{k_2}{2}\right)^2}, \frac{2k_1}{v} + 3\sqrt{k_1^2 + \left(\frac{k_2}{2}\right)^2} \right), \tag{12}$$

let

$$t_0 = \frac{2k_1}{v} + 2\sqrt{k_1^2 + \left(\frac{k_2}{2}\right)^2} \tag{13}$$

the equation of motion at this period is as follows:

$$\begin{cases} x = x_0 + k_2 - \dfrac{k_2 \cdot v \cdot (t - t_0)}{2\sqrt{k_1^2 + 2}}, \\ y = y_0 + \dfrac{k_1 \cdot v \cdot (t - t_0)}{\sqrt{k_1^2 + (k_2/2)^2}} \end{cases} \tag{14}$$

(6) Movement equation along the FA direction: when a drone moves in the FA direction, the task time is represented as

$$t \in \left[\frac{2k_1}{v} + 3\sqrt{k_1^2 + \left(\frac{k_2}{2}\right)^2}, \frac{2k_1}{v} + 4\sqrt{k_1^2 + \left(\frac{k_2}{2}\right)^2} \right] \tag{15}$$

let

$$t_0 = \frac{2k_1}{v} + 3\sqrt{k_1^2 + \left(\frac{k_2}{2}\right)^2}, \tag{16}$$

the equation of motion at this period is as follows:

$$\begin{cases} x = x_0 + \dfrac{k_2}{2} - \dfrac{k_2 \cdot v \cdot (t - t_0)}{2\sqrt{k_1^2 + (k_2/2)^2}}, \\ y = y_0 + k_1 - \dfrac{k_1 \cdot v \cdot (t - t_0)}{\sqrt{k_1^2 + (k_2/2)^2}} \end{cases} \tag{17}$$

Therefore, after the time $(2k_1/v) + 4\sqrt{k_1^2 + (k_2/2)^2}$, the drone completes the task of detection, perception,

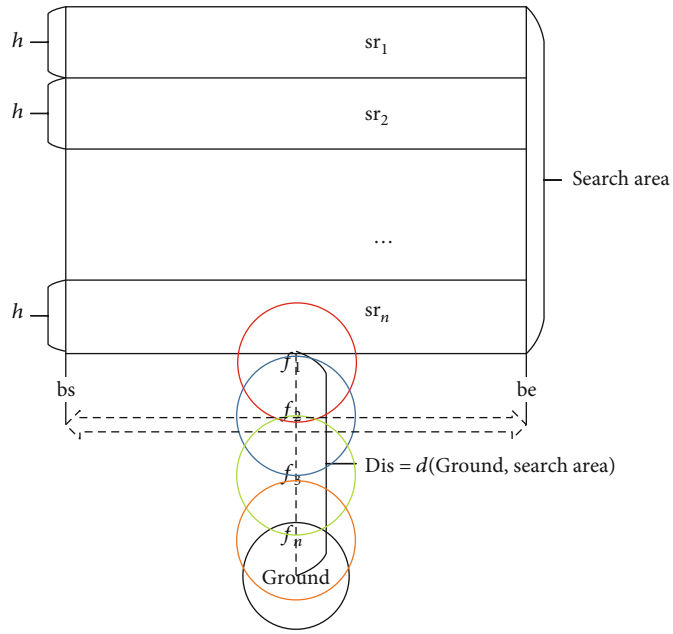

Figure 3: The setting of ferry UAVs. f_1-f_n are ferry UAVs, and they move back between bs and be with the same speed.

and collection of messages in the entire SSA. In addition, due to interference from outdoor geography, signals, and other factors, the drone may need to repeat the investigation after a round of investigation to ensure the accuracy and completeness of messages.

3.1.3. Division Rules of Area Layers. In this paper, the detection area is a rectangle, and the height and width of the task area are represented by H_{all} and W_{all}. The task area is divided into multiple area layers according to the hierarchical structure, so that the drone is routed according to the hierarchical increment method, as shown in Figure 3. For each area layer, in order to ensure that the UAVs in the area layer can communicate, the division of the area layer satisfies the following rules.

Rule 1. Let h be the height of AL and let Range be the maximum communication range of a UAV, then $h \leq \text{Range}$.

Rule 1 ensures that UAVs in the upper and lower ALs can transmit messages.

Rule 2. Let w and H_{all} be the width of the area layer and the height of the detection area and let Num(sub) be the number of ALs, then $\text{Num(sub)} \geq H_{\text{all}}/\text{Range}$.

Rule 2 can be calculated from Rule 1.

Rule 3. The rule of numbering ALs. ALs are numbered far and near according to the distance from the ground station.

Let sr_i be the No.i AL and let n be the number of ALs. According to Rule 3, shown in Figure 3, the AL farthest from the ground station is numbered as sr_1, and the area layer closest to the ground is numbered as sr_n, so that messages are transmitted in the direction of increasing area layer.

3.1.4. Message Transmission Method between Adjacent Area Layers—PB. Multiple searching UAVs are allocated in each AL to detect, sense, and collect messages. Messages are transmitted from the current AL to the next high AL. For each AL named sr_i and each searching UAV $m_i(j) \in \text{sr}_i$, we compare the distance of all the neighbors located in the moment, and select the next node $m_{i+1}(k)$ in sr_{i+1} that fulfills the following condition:

$$\begin{aligned} &\arg\ \min_j \quad d(m_i(j), m_{i+1}(k)) \\ &\text{subject to} \quad d(m_i(j), m_{i+1}(k)) \leq \text{Range}. \end{aligned} \tag{18}$$

In the formula, $d(m_i(j), m_{i+1}(k))$ is the geographical distance of node $m_i(j)$ to the node $m_{i+1}(k)$. $d(m_i(j), m_{i+1}(k)) < \text{Range}$ ensures that the drone in sr_i can establish connections with drones in sr_{i+1}. PB selects the closest neighbor in sr_{i+1} as the next node to reduce delay. The algorithm PB (*Popularity* Balance Method for UAVs in the same area layer) is shown as Algorithm 1.

As a result, messages in sr_i transfer along sr_i, sr_{i+1}, sr_{i+2}, $\cdots$, sr_n, and finally to the highest AL, which is named sr_n.

3.1.5. Setting Rules of Ferry UAVs. When there is a certain distance between the detection area and the ground station, the text [22] additionally uses ferry UAVs to move back and forth between the searching UAVs and the ground station to help the message transmission. When a drone uses a geographical routing method for message transmission, a large number of messages will be transmitted back and forth. This article resets the running rules of ferry UAVs, so that the message is still transmitted to the ground station in a hierarchical manner. The setting of the ferry UAV satisfies the following rules.

```
1:for m_i(j) in sr_i do
2:   procedure PB (m_i(j), next, M_data)      //Sending M_data from m_i(j) to next
3:      for a ∈ [1, Num(sr_{i+1})] do
4:         if d(m_i(j), m_{i+1}(a)) ≤ Range and d(m_i(j), m_{i+1}(a)) < d(m_i(j), m_{i+1}(k)) then
5:            k ← a
6:         end if
7:      end for
8:      FORWARDTo (m_{i+1}(k), M_data)      //Sending M_data to m_{i+1}(k)
9:   end procedure
10:end for
```

Algorithm 1: PB.

Rule 4. Numbering rules for ferry UAV. The ferries are numbered far and near according to the distance from the ground station.

Let f_i be the No.i ferry UAV and let n be the number of ferry UAVs. According to Rule 4 above, the ferry farthest from the ground station is numbered f_1, as shown in Figure 3, and ferries are numbered from the search area to Ground via $f_1, f_2, f_3, \cdots, f_n$ in order.

Rule 5. Let $d(G, \mathrm{SA})$ be the distance between the ground and SA, let R_g be the maximum sensing range of each searching UAV, and let R_f be the maximum communication range of each ferry, so the number of ferry UAVs $\mathrm{Num(ferry)}$ needs to satisfy the formula: $\mathrm{Num(ferry)} \times R_f > d(G, \mathrm{SA}) + R_g$.

According to Rule 5 above, f_n can establish a connection with searching UAVs in the highest AL sr_n during the task time, and messages can be transmitted to the ground via $f_1, f_2, f_3, \cdots, f_n$.

Rule 6. The operating rule of ferry UAVs. Each ferry moves back and forth along the width of SA.

According to Rule 6 above, shown in Figure 3, the ferry moves back and forth between the boundary bs and be. Ferry UAVs expand the communication range of SA, so that messages can reach the ground station via $f_1, f_2, f_3, \cdots, f_n$, and finally to Ground.

Rule 7. Distance rule between adjacent ferry UAVs. At any time t during the mission, the distance between adjacent ferries $d_t(f_i, f_{i+1})$ is always less than its maximum communication range R_f, that is, $\forall t, \exists i \in [1, \mathrm{Num(ferry)} - 1], d_t(f_i, f_{i+1}) \le R_f$.

According to Rule 7 above, the adjacent ferry UAVs remain connected; thus, messages can transmit to a higher-number ferry at all times.

Rule 8. Distance rule between ferry UAVs and ground. At some time t during the mission, the distance between the highest-number ferry f_n and ground G can be less than the ferry's maximum communication range R_f, that is, $\exists \mathrm{t}, d_t(f_n, G) \le R_f$.

According to Rule 8 above, the highest-number ferry UAV can be connected to the ground during the mission time, so that messages can be transmitted to the ground station.

3.1.6. Modeling the Popularity Balance of Searching UAVs. To evaluate the overheads associated with the detection tasks, we consider two aspects—the overhead of the message and overhead of the UAV. In terms of messages, we mainly consider time delay, which is the time from when the messages are perceived to the time it reaches the ground station. In terms of UAVs, the main cost is the battery. One one hand, UAVs need to fly to the required area and to move along a planned track to detect messages. One other hand, UAVs need to collect messages through sensors and need to transmit messages back to the ground station [27]. All these processes cost energy. The cost of flying is hard to avoid and each UAV similarly remains in the search and rescue scene. However, the different locations of the UAVs require them to use up different amounts energy to transmit messages because of the different number of messages passed on. Based on these, for the convenience of discussion, we analyse the unbalanced transmission of messages on different UAVs.

Sometimes, if an unsuitable transmission method is chosen to transmit messages, it can cause a "hot spot." A "hot spot" means that the number of messages passing on a node is much larger than the number of messages passing on other nodes. It spends a lot of energy on message transmission, and it could probably not have enough energy to complete the investigation task, which may bring unpredictable losses, so we should take measures to avoid a "hot spot" as much as possible [28].

"*Popularity*" is proposed to indicate the ratio of the relayed message number to the total message number. Based on geographic routing, messages are transmitted closer to the destination; thus, the number of messages passing through some drones closer to the ground is much larger than number of messages passing through drones far from the ground [29].

Therefore, for the entire UAV network, the *popularity* of all UAVs is definitely not balanced. So, in this paper, we only discuss the *popularity* degree of the searching UAVs in the

Table 1: Symbol description.

Symbol	Value
$m_i(j)$	No.j searching UAV in No.i AL
sr_i	No.i AL
$\mathrm{Num}(\mathrm{sr}_i)$	The number of searching UAVs in sr_i
$S(m_i(j))$	The total number of messages passing on all $m_i(j)$
$\overline{SN_i}$	Average number of all $S(m_i(j))$ in sr_i
FC_i	The *popularity* balance of searching UAVs in sr_i
$S_{\mathrm{collect}}(m_i(j))$	Total number of messages collected by $m_i(j)$
$S_{\mathrm{receive}}(m_i(j))$	Total number of messages received by $m_i(j)$
e	The number of messages collected per second for each searching UAV (s/sec)
T	Task duration (s)
$P(a, b)$	Probability of message transmission between UAV a and b
$\{m_i\}$	The set of searching UAVs in sr_i
{ferry}	The set of all ferry UAVs
{searching}	The set of all searching UAVs

same AL to analyze whether there is a "hot spot." Based on this, we use the variance FC_i to represent the *popularity* balance of searching UAVs in each AL. For the convenience of description, the relevant symbol representations are shown in Table 1.

The model of *popularity* balance of searching UAVs in sr_i is given as follows:

$$\mathrm{FC}_i = \sum_{j=1}^{\mathrm{Num}(\mathrm{sr}_i)} \left(S\left(m_i(j) - \overline{SN_i}\right)\right)^2. \tag{19}$$

The number of messages relayed on each searching UAV is the total number of messages collected and received from others, and $S(m_i(j))$ can be described as follows:

$$S(m_i(j)) = S_{\mathrm{collect}}(m_i(j)) + S_{\mathrm{receive}}(m_i(j)), \tag{20}$$

where $S_{\mathrm{collect}}(m_i(j))$ denotes the sum number of messages collected by $m_i(j)$ during task duration T:

$$S_{\mathrm{collect}}(m_i(j)) = e \times T. \tag{21}$$

Additionally, {others} represents the set of drones other than $m_i(j)$, and $P(o, m_i(j))$ represents the probability of message transmission between $o \in \{\mathrm{others}\}$ and $m_i(j)$; thus, $S_{\mathrm{receive}}(m_i(j))$ can be expressed through the following equation:

$$S_{\mathrm{receive}}(m_i(j)) = \sum_{o \in \{\mathrm{others}\}} S(o) \cdot P(o, m_i(j)). \tag{22}$$

Thus, the total number of messages passing on all searching UAVs in each AL $S(\mathrm{sr}_i)$ can fulfill the following condition:

$$S(\mathrm{sr}_i) = \sum_{j=1}^{\mathrm{Num}(\mathrm{sr}_i)} S(m_i(j)). \tag{23}$$

In addition, based on equation (23), the average messages $\overline{SN_i}$ in equation (19) can be expressed as follows:

$$\overline{SN_i} = \frac{S(\mathrm{sr}_i)}{\mathrm{Num}(\mathrm{sr}_i)}. \tag{24}$$

Obviously, it can be seen from equation (19) that the larger the value of FC_i, the more unbalanced the *popularity* of the drones and the more likely the "hot spot" appears. So in order to avoid the "hot spot," we hope that the total number of messages passing on different searching UAVs tends to be the same.

3.1.7. Modeling the Effect of Ping-Pong. The "Ping-pong effect" means that a message is transmitted from one node to another and then back to the node, that is, the transmission path of the message exists in a loop [30].

In order to analyze the proportion of messages in the UAV network that produces the ping-pong effect, we can simply express the number of messages in the loop in the message transmission as $\mathrm{Num}_{\mathrm{pp}}$ and the total number of received messages as $\mathrm{total}_{\mathrm{message}}$, then the ping-pong effect model can be expressed as follows:

$$\mathrm{PP} = \frac{\mathrm{Num}_{\mathrm{pp}}}{\mathrm{total}_{\mathrm{message}}}. \tag{25}$$

Obviously, it can be seen from the above formula that when the total number of received messages is the same, the more messages that have loops, the larger the proportion of the ping-pong effect.

3.2. Properties of the Models of Popularity Balance and Ping-Pong Effect. For the models of the *popularity* balance and ping-pong effect in Section 3.1, this section analyzes the characteristics of PB, $\mathrm{DTN}_{\mathrm{geo}}$, $\mathrm{DTN}_{\mathrm{load}}$, and $\mathrm{DTN}_{\mathrm{close}}$ methods to obtain the following series of properties.

Property 1. For a certain layer sr_1 in PB, $S(m_1(j)) = e \times t$, $j \in Num(\mathrm{sr}_1)$.

Proof. PB causes messages to be transmitted to a higher-numbered AL. The drones in the lowest AL sr_1 do not receive messages from other ALs, that is, for $m_i(j)$ in sr_1, $\forall o \in \{\mathrm{others}\}$, $P(o, m_i(j)) = 0$, so equation (22) can be converted as follows:

$$S_{\mathrm{receive}}(m_1(j)) = 0. \tag{26}$$

Therefore, equation (20) can be simplified as $S(m_1(j)) = S_{\mathrm{collect}}(m_1(j)) = e \times t$.

Property 2. For a certain layer sr_1 in PB, $\overline{SN_1} = e \times t$.

Proof. According to Property 1, when $i = 0$, equation (23) can be simplified as follows:

$$\overline{SN_1} = \frac{\mathrm{Num}(\mathrm{sr}_1) \times e \times t}{\mathrm{Num}(\mathrm{sr}_1)} = \mathrm{e} \times \mathrm{t}. \tag{27}$$

Property 3. Let $\mathrm{FC}_1(\mathrm{PB})$ be the situation of *popularity* balance in sr_1 for PB, and it can be calculated that $\mathrm{FC}_1(\mathrm{PB}) = 0$.

Proof. According to Properties 1 and 2, equation (19) can be simplified as follows:

$$\mathrm{FC}_1(\mathrm{PB}) = \sum_{j=1}^{\mathrm{Num}(\mathrm{sr}_1)} (e \times t - e \times t)^2 = 0. \tag{28}$$

Property 4. For PB,$\forall k \in [1, \mathrm{Num}(\mathrm{sr}_i)]$, $S(m_i(k)) \approx e \times t \times i$.

Proof.

(1) When $i = 1$, according to Property 1, we can get the following:

$$\forall k \in [1, \mathrm{Num}(\mathrm{sr}_1)], S(m_1(k)) = e \times t. \tag{29}$$

(2) Analyze the result when $i \neq 1$

According to design requirement (1) of the search and rescue model in Section 3.1, it can be deduced that

$$\forall i, j \in [1, n], \mathrm{Num}(\mathrm{sr}_i) = \mathrm{Num}\left(\mathrm{sr}_j\right). \tag{30}$$

Since messages are transmitted in the direction of the higher-numbered AL, the message in this area layer is only transmitted to the next higher AL, so for $m_i(j)$ in sr_i, $\{\mathrm{others}\}$ in equation (22) can be expressed as

$$\{\mathrm{others}\} = \{m_{i-1}\}, \tag{31}$$

where $\{m_{i-1}\}$ represents the set of all searching UAVs in sr_i.

Thus, equation (22) can be simplified as follows:

$$S(m_i(\mathrm{j})) = \mathrm{e} \times \mathrm{t} + \sum_{o}^{\{m_{i-1}\}} S(o) \cdot P(\mathrm{o}, m_i(\mathrm{j})). \tag{32}$$

In addition, according to design requirements (2) and (3) of the search and rescue model in Section 3.1, we can analyze that any drone in sr_i has a similar probability of message transmission with other drones, which can be expressed as

$$\begin{aligned} &\forall x, y \in [1, \mathrm{Num}(\mathrm{sr}_i)], \sum_{o}^{\{m_{i-1}\}} S(o) \cdot P(o, m_i(x)) \\ &\approx \sum_{o}^{\{m_{i-1}\}} S(o) \cdot P(o, m_i(y)). \end{aligned} \tag{33}$$

From equations (32) and (33), it can be deduced that

$$\forall x, y \in [1, \mathrm{Num}(sr_i)], S(m_i(x)) \approx S(m_i(y)). \tag{34}$$

From (1), $i = 1$, $\forall k \in [1, \mathrm{Num}(\mathrm{sr}_1)]$, $S(m_1(k)) = e \times t$; when not considering conditions such as packet loss, it can be deduced that

$$\begin{aligned} &S(m_2(k)) \approx e \times t + \overline{SN_1} = e \times t + e \times t = 2 \times e \times t, \\ &S(m_3(k)) \approx e \times t + \overline{SN_2} = e \times t + 2 \times e \times t = 3 \times e \times t. \end{aligned} \tag{35}$$

Thus, it can be obtained through mathematics that

$$S \approx e \times t \times i, \quad i \neq 1. \tag{36}$$

The following conclusion can be drawn from the discussion when $i = 1$ and $i \neq 1$:

$$\forall k \in [1, \mathrm{Num}(\mathrm{sr}_i)], S(m_i(k)) \approx e \times t \times i. \tag{37}$$

where $\{\mathrm{searching}\}$ represents the set of all searching UAVs and $\{\mathrm{ferry}\}$ represents the set of all ferry UAVs.

Property 5. For PB, it can be deduced that $\forall i \in (1, \mathrm{Num}(\mathrm{sub})]$, $\overline{SN_i} \approx e \times t \times i$.

Proof. According to Property 4, equation (23) can be simplified as follows:

$$\overline{SN_i} \approx \frac{\mathrm{Num}(\mathrm{sr}_i) \times e \times t \times i}{\mathrm{Num}(\mathrm{sr}_i)} = e \times t \times i. \tag{38}$$

Property 6. Let $\mathrm{FC}_i(\mathrm{PB})$ be the situation of *popularity* balance in sr_i, $i \in [1, \mathrm{Num}(\mathrm{sub})]$, and it can be deduced that $\mathrm{FC}_i(\mathrm{PB}) \approx 0$.

Proof. According to Property 4 and Property 5, equation (19) can be simplified as follows:

$$\mathrm{FC}_i(\mathrm{PB}) \approx \sum_{j=1}^{\mathrm{Num}(\mathrm{sr}_i)} (e \times t \times i - e \times t \times i)^2 = 0. \tag{39}$$

Property 7. For a certain layer sr_i, $i \in [1, \mathrm{Num}(\mathrm{sub})]$ in $\mathrm{DTN}_{\mathrm{geo}}$, $\mathrm{DTN}_{\mathrm{close}}$, and $\mathrm{DTN}_{\mathrm{load}}$, it can be deduced that

$$S(m_i(j)) = e \times t + \sum_{o}^{\{\mathrm{searching}\} - m_i(j) + \{\mathrm{ferry}\}} S(o) \cdot P(o, m_i(j)), \tag{40}$$

where $\{\mathrm{searching}\}$ is the set of all searching UAVs and $\{\mathrm{ferry}\}$ is all ferry UAVs.

Proof. Since ferries move back and forth between the ground and searching UAVs, each searching UAV receives the number of messages transmitted from the other searching UAVs and ferry UAVs. Therefore, for $m_i(j)$ in sr_i, $\{\mathrm{others}\}$ in equation (22) can be expressed as

$$\{\text{others}\} = \{\text{searching}\} - m_i(j) + \{\text{ferry}\}, \quad (41)$$

Therefore, equation (22) can be simplified as

$$S(m_i(j)) = e \times t + \sum_{o}^{\{\text{searching}\}-m_i(j)+\{ferry\}} S(o) \cdot P(o, m_i(j)). \quad (42)$$

Property 8. For DTN_{geo}, $\text{DTN}_{\text{close}}$, and DTN_{load}, it can be deduced that $S(m_i(a)) \gg S(m_i(b))$, $(a \in HA, b \notin HA)$, where HA represents a "hot area" that means some area nearer the destination than others in each AL.

Proof. For DTN_{geo}, $\text{DTN}_{\text{close}}$, and DTN_{load}, any drone selects the neighbor node closest to the ground as the next node. Each time that $m_i(k)$ selects the next node, the drone always select some node with a higher probability [31]; it can be expressed as follows:

$$P(m_i(k), a) \gg P(m_i(k), b) \quad (a \in HA, b \notin HA). \quad (43)$$

According to Property 7 and formula (43), it can be deduced that

$$S(m_i(a)) \gg S(m_i(b)). \quad (44)$$

Property 9. Let $\text{FC}_i(\text{DTN}_{\text{geo}})$, $\text{FC}_i(\text{DTN}_{\text{close}})$, and $\text{FC}_i(\text{DTN}_{\text{load}})$ be the situation of *popularity* balance of DTN_{geo}, $\text{DTN}_{\text{close}}$, DTN_{load} sr_i, $i \in [1, \text{Num(sub)}]$ in the three schemes; it can be calculated that $\text{FC}_i(\text{DTN}_{\text{geo}}) \gg 0$, $\text{FC}_i(\text{DTN}_{\text{close}}) \gg 0$, and $\text{FC}_i(\text{DTN}_{\text{load}}) \gg 0$.

Proof. According to Property 8, and with the characteristics of equation (19)—when values of $S(m_i(j))$ are not equal to each other and the difference is larger, the value FC_i is greater, and it can be deduced that

$$\begin{aligned} \text{FC}_i(\text{DTN}_{\text{geo}}) &\gg 0, \\ \text{FC}_i(\text{DTN}_{\text{close}}) &\gg 0, \\ \text{FC}_i(\text{DTN}_{\text{load}}) &\gg 0. \end{aligned} \quad (45)$$

Property 10. For PB, $\text{Num}_{\text{pp}} = 0$.

Proof. All messages are transmitted via $\text{sr}_i, \text{sr}_{i+1}, \text{sr}_{i+2}, \cdots, \text{sr}_n, f(1), f(2), \cdots, f(n), G$, so there is no loop in the transmission path; thus, $\text{Num}_{\mathbf{pp}} = 0$.

Property 11. For DTN_{geo}, $\text{DTN}_{\text{close}}$, and DTN_{load}, $\text{Num}_{\text{pp}} > 0$.

Proof. DTN_{geo} transmits messages to the neighbor node closest to the ground, and because ferries move back and forth between searching UAVs and the ground, the distance between ferries and the ground always changes. If one ferry is closest to the ground station in the neighbor node, messages will be transmitted to that at the time. If one ferry is far away from the ground, the messages will be retransmitted back; there exists a loop in the transmission path, so $\text{Num}_{\mathbf{pp}} > 0$.

3.3. Comparison of PB with DTN_{geo}, DTN_{load}, and DTN_{close} in the Popularity Balance and Ping-Pong Effect

Theorem 1. *$FC_i(PB) < FC_i(DTN_{geo})$.*

Proof. According to Property 6 and Property 9, it can be deduced that

$$\text{FC}_i(\text{PB}) < \text{FC}_i\left(\text{DTN}_{\text{geo}}\right). \quad (46)$$

Theorem 2. *Let $PP(PB)$ and $PP(DTN_{geo})$ be the ping-pong effect ratio of PB and DTN_{geo}, respectively, then $PP(PB) < PP(DTN_{geo})$.*

Proof. According to Property 10 and Property 11, with the same value of $\text{total}_{\text{message}}$, equation (25) can be deduced as follows:

$$\text{PP}(\text{PB}) < \text{PP}\left(\text{DTN}_{\text{geo}}\right). \quad (47)$$

Theorem 3. *$FC_i(PB) < FC_i(DTN_{close})$.*

Proof. According to Property 6 and Property 9, it can be deduced that

$$\text{FC}_i(\text{PB}) < \text{FC}_i(\text{DTN}_{\text{close}}). \quad (48)$$

Theorem 4. *Let $PP(PB)$ and $PP(DTN_{close})$ be the ping-pong effect ratio of PB and DTN_{close}, respectively, then $PP(PB) < PP(DTN_{close})$.*

Proof. According to Property 10 and Property 11, with the same value of $\text{total}_{\text{message}}$, equation (25) can be deduced as follows:

$$\text{PP}(\text{PB}) < \text{PP}(\text{DTN}_{\text{close}}). \quad (49)$$

Theorem 5. *$FC_i(PB) < FC_i(DTN_{load})$.*

Proof. According to Property 6 and Property 9, it can be deduced that

$$\text{FC}_i(\text{PB}) < \text{FC}_i(\text{DTN}_{load}). \quad (50)$$

Theorem 6. *Let $PP(PB)$ and $PP(DTN_{load})$ be the ping-pong effect ratio of PB and DTN_{load}, respectively, then $PP(PB) < PP(DTN_{load})$.*

Proof. According to Property 10 and Property 11, with the same value of $\text{total}_{\text{message}}$, equation (25) can be deduced as follows:

$$\text{PP}(\text{PB}) < \text{PP}(\text{DTN}_{load}). \quad (51)$$

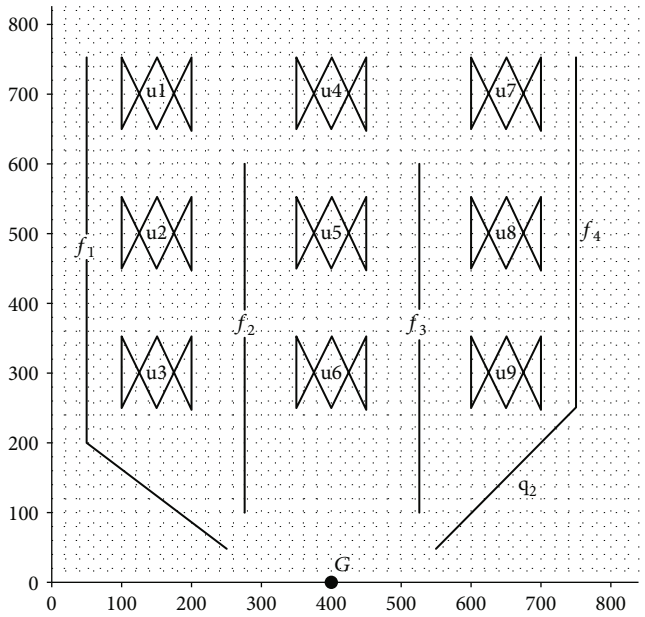

Figure 4: Simulation scenario of DTN_{geo}, DTN_{close}, and DTN_{load} with a ground station and the trajectories of four ferry UAVs (f_1-f_4) and nine searching UAVs (u1-u9),

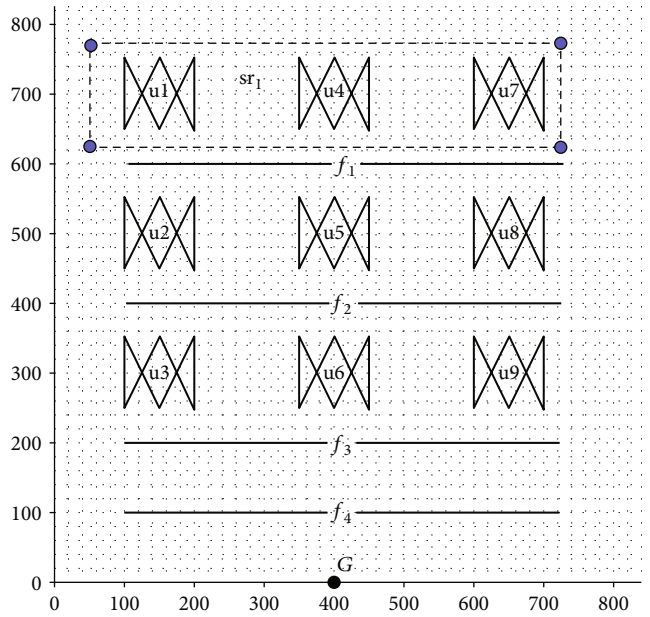

Figure 5: Simulation scenario of PB with a ground station and the trajectories of four ferry UAVs (f_1-f_4) and nine searching UAVs (u1-u9); u1, u4, and u7 are in the same AL named sr_1.

3.4. Comparison of PB with DTN_{geo}, DTN_{load}, and DTN_{close} in the Complexity of the Algorithm

Theorem 7. *Let $O_{PB}, O_{DTN_{geo}}, O_{DTN_{load}}$ and $O_{DTN_{close}}$ be the complexity of PB, DTN_{geo}, DTN_{load}, and DTN_{close}, then $O_{PB} < O_{DTN_{geo}} = O_{DTN_{close}} = O_{DTN_{load}}$.*

Proof. For PB, since each drone always selects the drone that is closer to itself in the next area layer for transmission of messages, it only needs to calculate distances of drones in the next area layer. For n drones in the whole system, if the number of drones in each area layer is k, the complexity of PB $O_{PB} = O(n * k)$, where $k < n$.

For DTN_{geo}, DTN_{load}, and DTN_{close}, when each drone chooses a message transmission object, it needs to calculate the distances of all the other drones. For n drones in the whole system, the complexity of DTN_{geo}, DTN_{load}, and DTN_{close} $O_{DTN_{geo}} = O_{DTN_{close}} = O_{DTN_{load}} = O(n^2)$.

Therefore, $O_{PB} < O_{DTN_{geo}} = O_{DTN_{close}} = O_{DTN_{load}}$, that is PB has lower complexity than DTN_{geo}, DTN_{load}, and DTN_{close}.

4. Simulation Design and Results

4.1. Simulation Setup. In this paper, PB, DTN_{geo}, DTN_{close}, and DTN_{load} are implemented in the ONE simulator [32]. In order to compare the ratio of *popularity* and ping-pong effect of the three schemes, we construct the simulation scenario with the maximum number of drones in [22].

The trajectories of UAVs of DTN_{geo}, DTN_{close}, and DTN_{load} are shown in Figure 4. The scene consists of a basic ground station (G), up to nine searching UAVs (u1-u0), and four ferry UAVs (f_1-f_4). f_1-f_4 moves back and forth between u1 and u9 and ground station G, and f_1-f_4 and f_2-f_3 always maintain reverse motion. The detection subarea of each searching UAV is 200 m × 200 m, which defines the service and message collection area of each drone.

The trajectories of UAVs in PB are shown in Figure 5, where u1/u4/u7, u2/u5/u8, and u3/u6/u9 are, respectively, located in sr_1, sr_2, and sr_3. And the distance between the detection area and the ground station $d(G, \mathrm{SA})$ is 200 m, the sensing radius of the searching UAV R_g is 100 m, and the sensing radius of the ferry UAV R_f is 200 m. According to Rule 2, Rule 3, and Rule 7 of setting the rules of ferry UAVs in Section 3.1, two ferries are planned for message transmission between sr_3 and G, and we also define the distance between adjacent ferries, that is, the distance is always 100 m. In addition, in order to be consistent with the number of ferry UAVs of the other three methods, we also plan f_1 and f_2 between the regional layers to ensure link quality of the wireless communication of drones.

The specific experimental parameters of this paper are shown in Table 2.

By comparing the performance hazard caused by the unbalanced *popularity* of drones, we analyse that the more messages generated per second, the more likely the network is to generate congestion, and drones will consume more energy in message transmission. Therefore, the experimental variable in this paper that we selected is the rate of messages generated per second, and we selected different message rates (1/2/3/4/5/10/15) to analyse the results of different algorithms. In addition, in order to analyse the influence of the size of the search area on the results, we also use different areas (800m × (200m/800m) × (600m/800m) × (800m/800m) × 1000m), separately using (7/10/13/16) drones.

Table 2: Experimental parameters.

Parameters	Values
Height of each AL	200 m
$d(G, \mathrm{SA})$	200 m
Number of Ground	1
Number of UAVs (searching/ferry)	16 (12/4)
Mission time	8 min
Speed of all UAVs	4.5 m/s
Transmission range of all UAVs	200 m
Sensing radius of searching UAV R_g	100 m
The size of each message	1.4 kb

Additionally, we only consider a routing algorithm in this paper. And reliable transmission is completed by relevant protocols in the physical layer and the data link layer, so there is no excessive consideration of mechanisms such as message retransmission and packet acknowledgment. Then, the natural problem of link protocols cannot guarantee that all messages reach the destination node successfully, but the number of messages' loss rate varies depending on the routing algorithm selected. So, we set the indicator "delivery rate" to evaluate the value of messages that succeed in reaching the destination. Moreover, to evaluate algorithms in different aspects, the following metrics are used to evaluate the performance of these algorithms:

(1) *Popularity*: that is, the ratio of the relayed message number to the total message number

(2) *Ping-pong effect ratio*: that is, the number of messages that have a loop in path transmission out of the total number of messages

(3) *Delivery ratio*: that is, the number of messages that have been successfully transmitted to the ground out of the total number of messages

(4) *Delay*: that is, the communication delay generated from the node to the destination

(5) *Hop count*: that is, the sum of hops a message passes through until it reaches the destination

4.2. Discussion of Results

4.2.1. Comparing the Popularity. In order to evaluate the degree of *popularity* in PB, $\mathrm{DTN}_{\mathrm{geo}}$, $\mathrm{DTN}_{\mathrm{close}}$, and $\mathrm{DTN}_{\mathrm{load}}$ schemes, we select the experimental parameters in [22] for comparison, that is, the rate of messages generated per second is 5. As shown in Figure 6, PB and UAVs in the same area layer (such as u1/u4/u7, u2/u5/u8, and u3/u6/u9) have a similar degree, while the $\mathrm{DTN}_{\mathrm{geo}}$, $\mathrm{DTN}_{\mathrm{close}}$, and $\mathrm{DTN}_{\mathrm{load}}$ methods all have obvious "hot spots" shown as u6. The reason for the results is that all the methods above are based on geographical routing, making the message closer to the ground station, and PB transmits messages to the area layer closer to the destination node instead of the closer node. Accordingly, messages' delivery direction is replaced by "point-to-point closer" to "point-to-face closer", avoiding u6 which is the closest to the ground accepting a large number of relayed messages. In addition, Figure 6 also shows that the degree of f_1-f_4 in the PB method is greater than that of the $\mathrm{DTN}_{\mathrm{geo}}$, $\mathrm{DTN}_{\mathrm{close}}$, and $\mathrm{DTN}_{\mathrm{load}}$ methods, indicating that PB plays a better role of ferry UAVs as a relay.

In addition, Figure 6 not only shows that the degree of u6 is much larger than that of all other searching UAVs but it also indicates that as the number of layers in the area increases, the degree of heat of the drone increases. So we set the different rates of the messages generated per time, and compared the FC_3 of each method by calculating the value of formula (19). As shown in Figure 7, the experimental results show that the larger the message rate generated per time, the larger the value of FC_3 and FC_3 $(DTN_{geo}) > \mathrm{FC}_3(\mathrm{PB})$, $\mathrm{FC}_i(\mathrm{LB}) < \mathrm{FC}_i(\mathrm{DTN}_{\mathrm{close}})$, and $\mathrm{FC}_i(\mathrm{LB}) < \mathrm{FC}_i(\mathrm{DTN}_{\mathrm{load}})$ with all different rates, which is consistent with Theorems 1, 3, and 5 in Section 3.3.

4.2.2. Comparing the Ping-Pong Effect Ratio. In Section 4.2.1, we selected one special experimental parameter to analyze the *popularity* of each UAV of different algorithms. In this section, we experiment on the impact of different rates of messages generated per time and the different numbers of UAVs on a ping-pong effect ratio. The result is shown in Figures 8 and 9. Figure 8 shows the influence of the rate of the messages generated per time on a ping-pong effect ratio, and Figure 9 shows the influence of the number of UAVs on a ping-pong effect ratio.

Both Figures 8 and 9 show that the degree of the PB method is always 0, and those of $\mathrm{DTN}_{\mathrm{geo}}$, $\mathrm{DTN}_{\mathrm{close}}$, and $\mathrm{DTN}_{\mathrm{load}}$ are always greater than 30%. PB can effectively avoid the ping-pong effect, which is consistent with Theorems 2, 4, and 6 in Section 3.3.

The reason for the appearance of the ping-pong effect is mainly that the $\mathrm{DTN}_{\mathrm{geo}}$, $\mathrm{DTN}_{\mathrm{close}}$, and $\mathrm{DTN}_{\mathrm{load}}$ methods enable messages to be point-to-point closer to the destination, and the distance between ferries and the ground is changing during mission time. For example, at a certain time, when a UAV calculates the distance between all neighbours and the ground station, if one ferry is the closest, the drone will transmit messages to the ferry. At some point later, when the ferry UAV calculates the distance between all neighbours and the ground and the distance between the UAV and the ground station is the closest, the message will be returned. PB replaces the relay between searching UAVs and the ground station by replacing the ferry UAVs as the relay between the highest regional layer and the ground station, so that messages are always toward the area layer closer to the ground. Thus, it can avoid back and forth transmission of messages, avoiding poor performance caused by the ping-pong effect.

4.2.3. Comparing the Delivery Ratio. In this section, we examine the impact of the different rates of the messages generated per time and the different numbers of UAVs on the delivery ratio. The results are shown in Figures 10 and 11. Figure 10

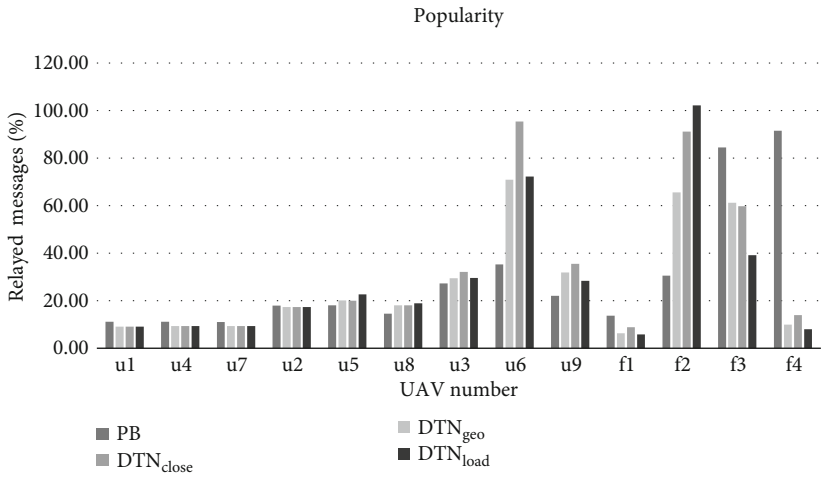

Figure 6: The *popularity* of different methods.

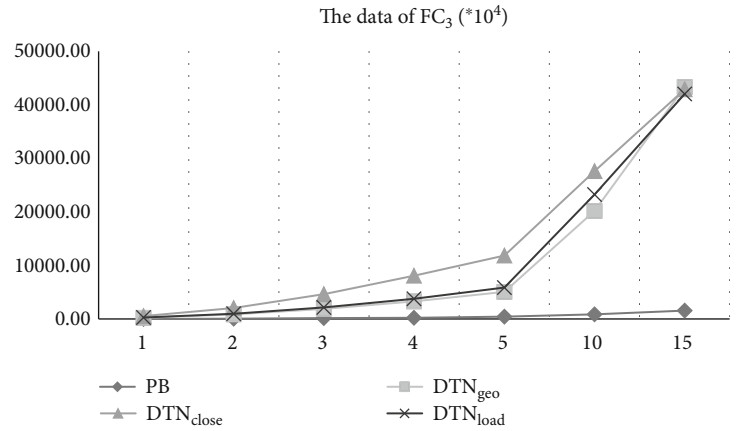

Figure 7: Influence of the rate of the messages generated per time on FC$_3$.

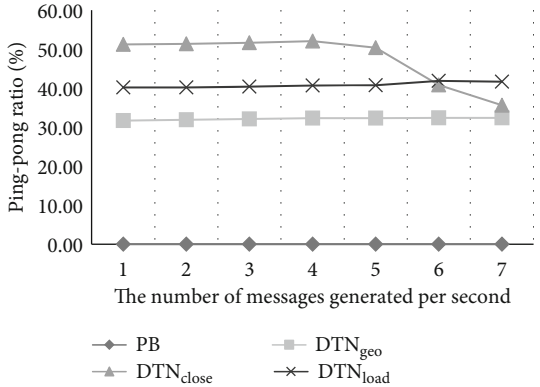

Figure 8: Influence of the rate of the messages generated per time on a ping-pong effect ratio.

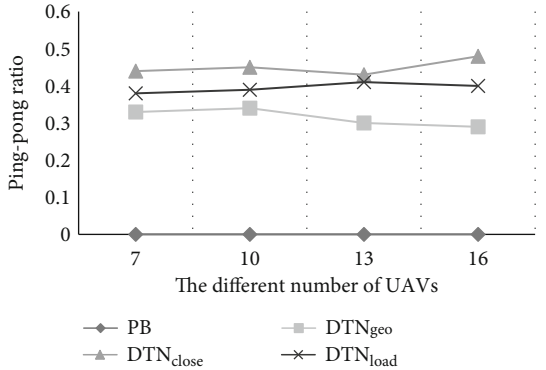

Figure 9: Influence of the number of UAVs on a ping-pong effect ratio.

shows the influence of the rate of the messages generated per time on the delivery ratio, and Figure 11 shows the influence of the number of UAVs on the delivery ratio.

Both Figures 10 and 11 show that PB has a certain improvement in the delivery rate compared with DTN$_{geo}$, DTN$_{close}$, and DTN$_{load}$. The reason for the result is that PB balances the *popularity* of UAVs in the same area layer and avoids the appearance of a "hot spot," thereby reducing the problem of packet loss due to congestion, so as to improve the delivery ratio.

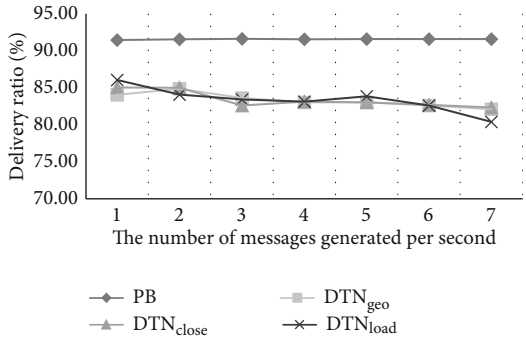

Figure 10: Influence of the rate of the messages generated per time on the delivery ratio.

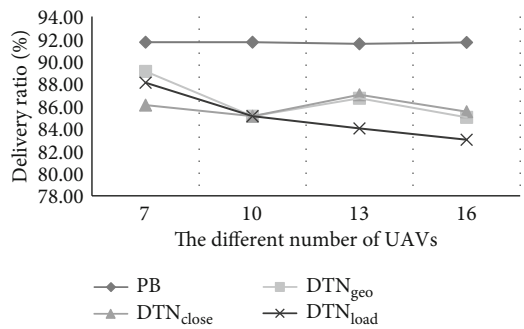

Figure 11: Influence of the number of UAVs on the delivery ratio.

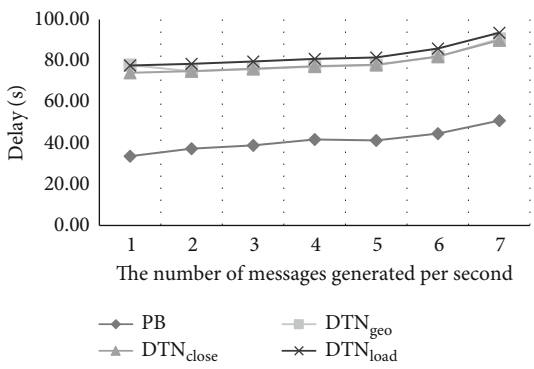

Figure 12: Influence of the rate of the messages generated per time on delay.

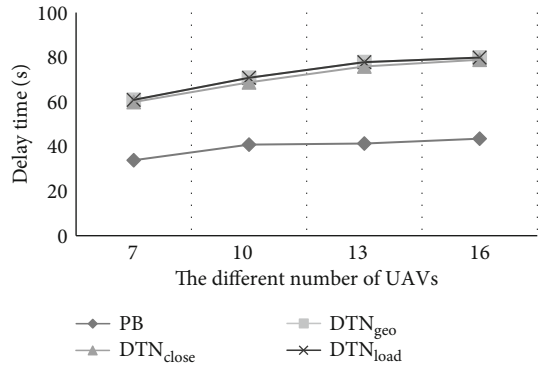

Figure 13: Influence of the number of UAVs on delay.

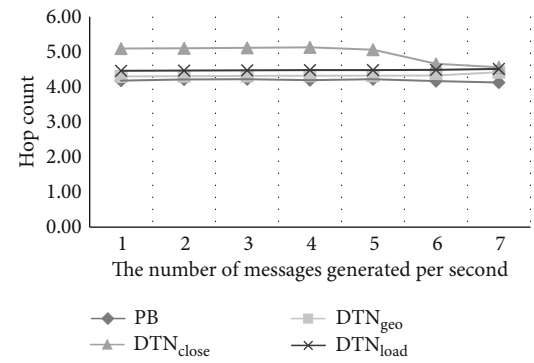

Figure 14: Influence of the rate of the messages generated per time on hop count.

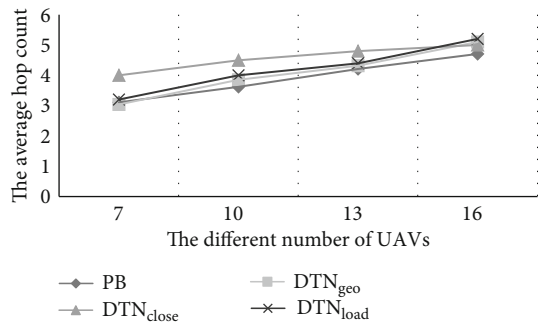

Figure 15: Influence of the number of UAVs on hop count.

4.2.4. Comparing the Delay. In this section, we examine the impact of the different rates of the messages generated per time and the different numbers of UAVs on delay. The result is shown in Figures 12 and 13. Figure 12 shows the influence of the rate of the messages generated per time on delay, and Figure 13 shows the influence of the number of UAVs on delay.

Both Figures 12 and 13 show that PB has a significant improvement on delay compared to DTN$_{geo}$, DTN$_{close}$, and DTN$_{load}$, reducing from about 80 s to about 40 s. The reason for the result is that PB avoids the appearance of a "hot spot," then reduces the waiting time for messages on the "hot spot." On the other hand, replanning the running rules of ferry UAVs avoids the ping-pong effect, so as to reduce unnecessary back-and-forth transmission time of messages, thereby reducing delay.

4.2.5. Comparing the Hop Count. In this section, we examined the impact of the different rates of the messages generated per time and the different numbers of UAVs on hop count. The result is shown in Figures 14 and 15. Figure 14 shows the influence of the rate of the messages generated per time on hop count, and Figure 15 shows the influence of the number of UAVs on hop count.

Both Figures 14 and 15 show that PB has a slight decrease in hop count compared to DTN$_{geo}$, DTN$_{close}$, and DTN$_{load}$. Although the hop count in the DTN$_{close}$ has a decrease with the increase in the number of messages generated per second,

it is still slightly higher than PB. The reason for the result is that PB replans the trajectory of ferry UAVs, so as to avoid the effect of the ping-pong effect, thereby reducing the unnecessary hops caused by the ping-pong effect.

5. Conclusion

PB, a message transmission method based on area layer division in UAV networks, is proposed in the paper.It divides the search area into multiple area layers and then transmits messages to the area layer closer to the ground based on the idea of geographical routing. The method transmits messages to the closer area layer instead of the closer node to the destination; thus, message delivery direction is replaced by "point-to-point closer" to "point-to-face closer." In addition, by resetting the operating rules, ferry UAVs are used as relays between the search area and the ground to replace the original motion between the searching UAVs and the ground, which effectively avoids a ping-pong effect, reducing the average number of hop counts and delay caused by unnecessary round-trip transmission. In the scenario simulation, delay is reduced from about 80 s to about 40 s. During the same mission time, the number of messages successfully transmitted to the ground is also increased. Because of less congestion, delivery ratio is also increased from over 80% to over 90%. Theoretical and experimental results both show that PB is superior to DTN_{geo}, DTN_{close}, and DTN_{load} in terms of *popularity*, ping-pong effect ratio, delivery ratio, delay, and hop count.

Data Availability

The data used to support the findings of this study are available from the corresponding author upon request.

Conflicts of Interest

The authors declare that there is no conflict of interest regarding the publication of this paper.

Acknowledgments

This work was supported in part by the Aeronautical Science Foundation of China under Grant 20165515001.

References

[1] B. Canis, *Unmanned aircraft systems (UAS): commercial outlook for a new industry*, Congressional Research Service Reports, 2015.

[2] D. Floreano and R. J. Wood, "Science, technology and the future of small autonomous drones," *Nature*, vol. 521, no. 7553, pp. 460–466, 2015.

[3] E. Yanmaz, S. Yahyanejad, B. Rinner, H. Hellwagner, and C. Bettstetter, "Drone networks: communications, coordination, and sensing," *Ad Hoc Networks*, vol. 68, article S1570870517301671, pp. 1–15, 2018.

[4] Y. Zhou, N. Cheng, N. Lu, and X. S. Shen, "Multi-UAV-aided networks: aerial-ground cooperative vehicular networking architecture," *IEEE Vehicular Technology Magazine*, vol. 10, no. 4, pp. 36–44, 2015.

[5] I. Guvenc, W. Saad, M. Bennis, C. Wietfeld, M. Ding, and L. Pike, "Wireless communications, networking, and positioning with unmanned aerial vehicles (guest editorial)," *IEEE Communications Magazine*, vol. 54, no. 5, pp. 24-25, 2016.

[6] R. Grodi, D. B. Rawat, and C. Bajracharya, "Performance evaluation of unmanned aerial vehicle ad hoc networks," in *SoutheastCon 2015*, pp. 1–4, Fort Lauderdale, FL, USA, 2015.

[7] M. K. Anantapalli and W. Li, "Multipath multihop routing analysis in mobile ad hoc networks," *Wireless Networks*, vol. 16, no. 1, article 116, pp. 79–94, 2010.

[8] M. Asadpour, D. Giustiniano, K. A. Hummel, and S. Egli, "UAV networks in rescue missions," in *Proceedings of the 8th ACM International Workshop on Wireless Network Testbeds, Experimental Evaluation & Characterization—WiNTECH '13*, pp. 91-92, Miami, Florida, USA, 2013.

[9] R. Jain, A. Puri, and R. Sengupta, "Geographical routing using partial information for wireless ad hoc networks," *IEEE Personal Communications*, vol. 8, no. 1, pp. 48–57, 2001.

[10] K. Fall and S. Farrell, "DTN: an architectural retrospective," *IEEE Journal on Selected Areas in Communications*, vol. 26, no. 5, pp. 828–836, 2008.

[11] A. Jimenez-Pacheco, D. Bouhired, Y. Gasser, J.-C. Zufferey, D. Floreano, and B. Rimoldi, "Implementation of a wireless mesh network of ultra light MAVs with dynamic routing," in *2012 IEEE Globecom Workshops*, pp. 1591–1596, Anaheim, CA, USA, 2012.

[12] H. Badis and K. Al Agha, "QOLSR, QoS routing for ad hoc wireless networks using OLSR," *European Transactions on Telecommunications*, vol. 16, no. 5, pp. 427–442, 2005.

[13] M. Asadpour, S. Egli, K. A. Hummel, and D. Giustiniano, "Routing in a fleet of micro aerial vehicles: first experimental insights," in *Proceedings of the Third ACM Workshop on Airborne Networks and Communications—AIRBORNE '14*, pp. 9-10, Philadelphia, PA, USA, 2014.

[14] I. Bekmezci, O. K. Sahingoz, and Ş. Temel, "Flying ad-hoc networks (FANETs): a survey," *Ad Hoc Networks*, vol. 11, no. 3, pp. 1254–1270, 2013.

[15] E. K. Cetinkaya, J. P. Rohrer, A. Jabbar et al., "Protocols for highly-dynamic airborne networks," in *Proceedings of the 18th Annual International Conference on Mobile Computing and Networking—Mobicom '12*, pp. 411–414, Istanbul, Turkey, 2012.

[16] B. B. Bista and D. B. Rawat, "EA-Epidemic: an energy aware epidemic-based routing protocol for delay tolerant networks," *Journal of Communications*, vol. 12, no. 6, pp. 304–311, 2017.

[17] X. Tie, A. Venkataramani, and A. Balasubramanian, "R3: robust replication routing in wireless networks with diverse connectivity characteristics," in *Proceedings of the 17th Annual International Conference on Mobile Computing and Networking—MobiCom '11*, Las Vegas, NV, USA, 2011.

[18] O. K. Sahingoz, "Networking models in flying ad-hoc networks (Fanets): concepts and challenges," *Journal of Intelligent & Robotic Systems*, vol. 74, no. 1-2, pp. 513–527, 2014.

[19] F. Lu, J.-B. Li, Y.-M. Song, and F.-S. Wang, "Location position and message delivery ratio based controlled epidemic routing for DTNs," *Journal of Chinese Computer Systems*, vol. 39, no. 5, 2018.

[20] R. Shirani, M. St-Hilaire, T. Kunz, Y. Zhou, J. Li, and L. Lamont, "Quadratic estimation of success probability of

greedy geographic forwarding in unmanned aeronautical ad-hoc networks," in *2012 IEEE 75th Vehicular Technology Conference (VTC Spring)*, pp. 1–5, Yokohama, Japan, 2012.

[21] J. Harri, P.-C. Cheng, J.-T. Weng, L.-C. Tung, M. Gerla, and K. Lee, "GeoDTN+Nav: a hybrid geographic and DTN routing with navigation assistance in urban vehicular networks," in *Proceedings of the First Annual International Symposium on Vehicular Computing Systems*, Dublin, Ireland, 2008.

[22] M. Asadpour, K. A. Hummel, D. Giustiniano, and S. Draskovic, "Route or carry: motion-driven packet forwarding in micro aerial vehicle networks," *IEEE Transactions on Mobile Computing*, vol. 16, no. 3, pp. 843–856, 2017.

[23] J. Scherer, S. Yahyanejad, S. Hayat et al., "An autonomous multi-UAV system for search and rescue," in *Proceedings of the First Workshop on Micro Aerial Vehicle Networks, Systems, and Applications for Civilian Use—DroNet '15*, pp. 33–38, Florence, Italy, 2015.

[24] L. Gupta, R. Jain, and G. Vaszkun, "Survey of important issues in UAV communication networks," *IEEE Communications Surveys & Tutorials*, vol. 18, no. 2, pp. 1123–1152, 2016.

[25] M. Asadpour, B. Van den Bergh, D. Giustiniano, K. Hummel, S. Pollin, and B. Plattner, "Micro aerial vehicle networks: an experimental analysis of challenges and opportunities," *IEEE Communications Magazine*, vol. 52, no. 7, pp. 141–149, 2014.

[26] R. Muzaffar and E. Yanmaz, "Trajectory-aware ad hoc routing protocol for micro aerial vehicle networks," in *IMAV 2014: International Micro Air Vehicle Conference and Competition 2014*, pp. 301–305, Delft, The Netherlands, August 2014.

[27] Q. Wu, Y. Zeng, and R. Zhang, "Joint trajectory and communication design for multi-UAV enabled wireless networks," *IEEE Transactions on Wireless Communications*, vol. 17, no. 3, pp. 2109–2121, 2018.

[28] J. Sánchez-García, J. M. García-Campos, S. L. Toral, D. G. Reina, and F. Barrero, "An intelligent strategy for tactical movements of UAVs in disaster scenarios," *International Journal of Distributed Sensor Networks*, vol. 12, no. 3, 2016.

[29] V. Sharma and R. Kumar, "A cooperative network framework for multi-UAV guided ground ad hoc networks," *Journal of Intelligent & Robotic Systems*, vol. 77, no. 3-4, pp. 629–652, 2015.

[30] D. T. Cole, P. Thompson, A. H. Goktogan, and S. Sukkarieh, "System development and demonstration of a cooperative UAV team for mapping and tracking," *The International Journal of Robotics Research*, vol. 29, no. 11, pp. 1371–1399, 2010.

[31] L. Yang, Y. Lu, L. Xiong, Y. Tao, and Y. Zhong, "A game theoretic approach for balancing energy consumption in clustered wireless sensor networks," *Sensors*, vol. 17, no. 11, article 2654, 2017.

[32] A. Keränen, J. Ott, and T. Kärkkäinen, "The ONE simulator for DTN protocol evaluation," in *Proceedings of the Second International ICST Conference on Simulation Tools and Techniques*, Rome, Italy, 2009.